Electronic Supplementary Information

EMISSION FROM THE STABLE BLATTER RADICAL

Georgina Karecla,[§] Paris Papagiorgis,[†] Nasia Panagi,[†] Georgia A. Zissimou,[§] Christos P. Constantinides,[§] Panayiotis A. Koutentis,[§] Grigorios Itskos,[†,*] Sophia C. Hayes[§,*]

S1. Theoretical Data at the DFT UB3LYP/6-311+G(d,p) Level of Theory

Table S1. Summary of Theoretical Data at the UB3LYP/6-311+G(d,p) Level of Theory

	Blatter radical
Uncorrected Energy (a.u.)	-896.896
ZPE	0.282
Scaled Energy (a.u.)	-896.617
Energy (eV)	-24398.198
Dipole (Debye)	3.116

S2. **Blatter Radical** Atom Coordinates at UB3LYP/6-311+G(d,p) Level of Theory

C(1)	-1.32796	0.32109	0.05027
C(2)	0.06490	2.14773	0.03581
C(3)	1.19855	1.29410	-0.06723
C(4)	1.95544	-1.07651	0.01133
C(5)	1.90142	-2.11972	-0.91453
C(6)	2.96786	-1.03717	0.97208
C(7)	2.87487	-3.11387	-0.88723
H(8)	1.09568	-2.14489	-1.63666
C(9)	3.93929	-2.03477	0.98886
H(10)	2.98300	-0.24352	1.70878
C(11)	3.89823	-3.07305	0.05941
H(12)	2.83384	-3.92146	-1.60910
H(13)	4.72038	-2.00653	1.73988
H(14)	4.65434	-3.84929	0.07751
C(15)	-2.70237	-0.25262	0.05400

C(16)	-3.81222	0.60207	0.04318
C(17)	-2.91145	-1.63876	0.06851
C(18)	-5.10292	0.08091	0.04428
H(19)	-3.64541	1.67103	0.03492
C(20)	-4.20328	-2.15567	0.06982
H(21)	-2.05615	-2.30129	0.08366
C(22)	-5.30388	-1.29872	0.05707
H(23)	-5.95350	0.75350	0.03495
H(24)	-4.35168	-3.22979	0.08325
H(25)	-6.30995	-1.70342	0.05850
C(26)	2.47806	1.83512	-0.25250
C(27)	0.27023	3.54053	0.01302
H(28)	-0.60280	4.17530	0.10366
C(29)	2.64277	3.21418	-0.28345
C(30)	1.54127	4.06808	-0.13815
H(31)	3.33230	1.18432	-0.37707
H(32)	3.63462	3.62676	-0.42625
H(33)	1.68359	5.14227	-0.15721
N(34)	0.93388	-0.07462	-0.00293
N(35)	-0.33384	-0.56903	-0.01928
N(36)	-1.20447	1.64782	0.12705

S3. Determination of the extinction coefficient of the Blatter radical in DCM solution

Figure S1 represents the absorbance of the most intense band at ~270 nm as a function of concentration for successive dilutions of a DCM solution of the radical. From Beer-Lambert's law, the slope of the curve provides the extinction coefficient for this transition, which was determined to be 6694 ± 92 $M^{-1}cm^{-1}$.
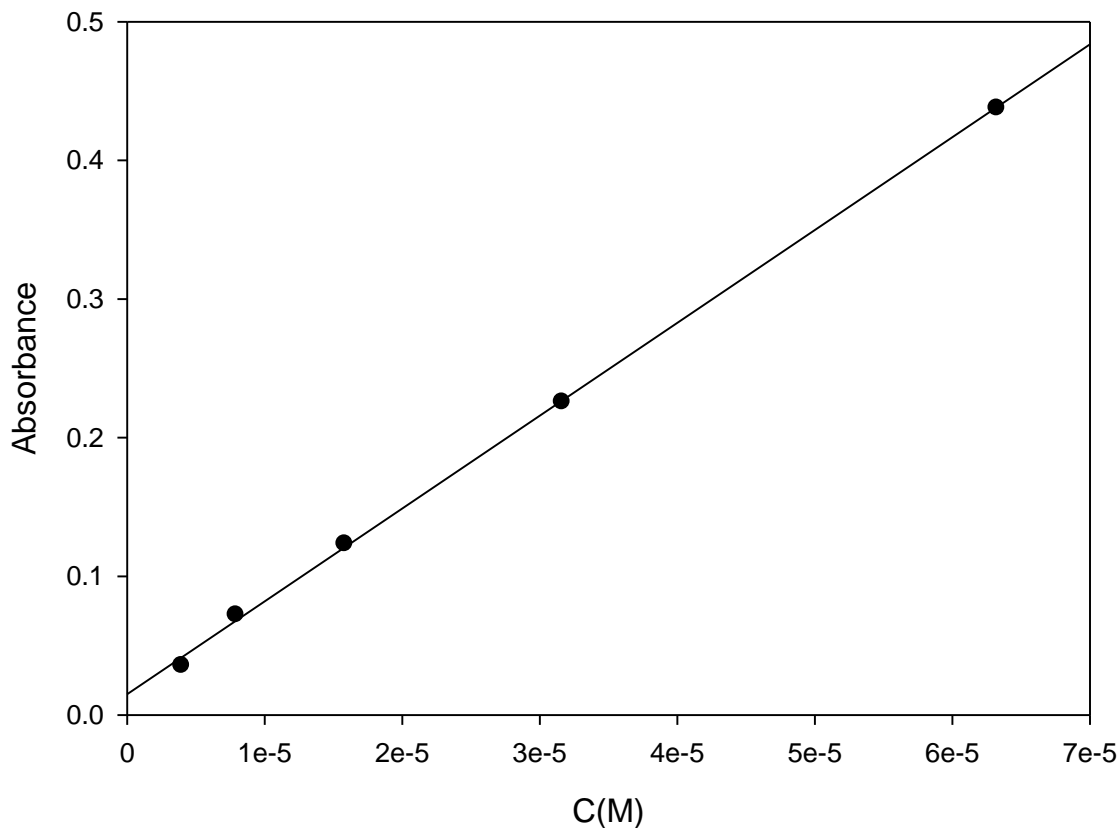

Figure S1. Absorbance of the 272 nm band of the Blatter radical in DCM as a function of concentration.
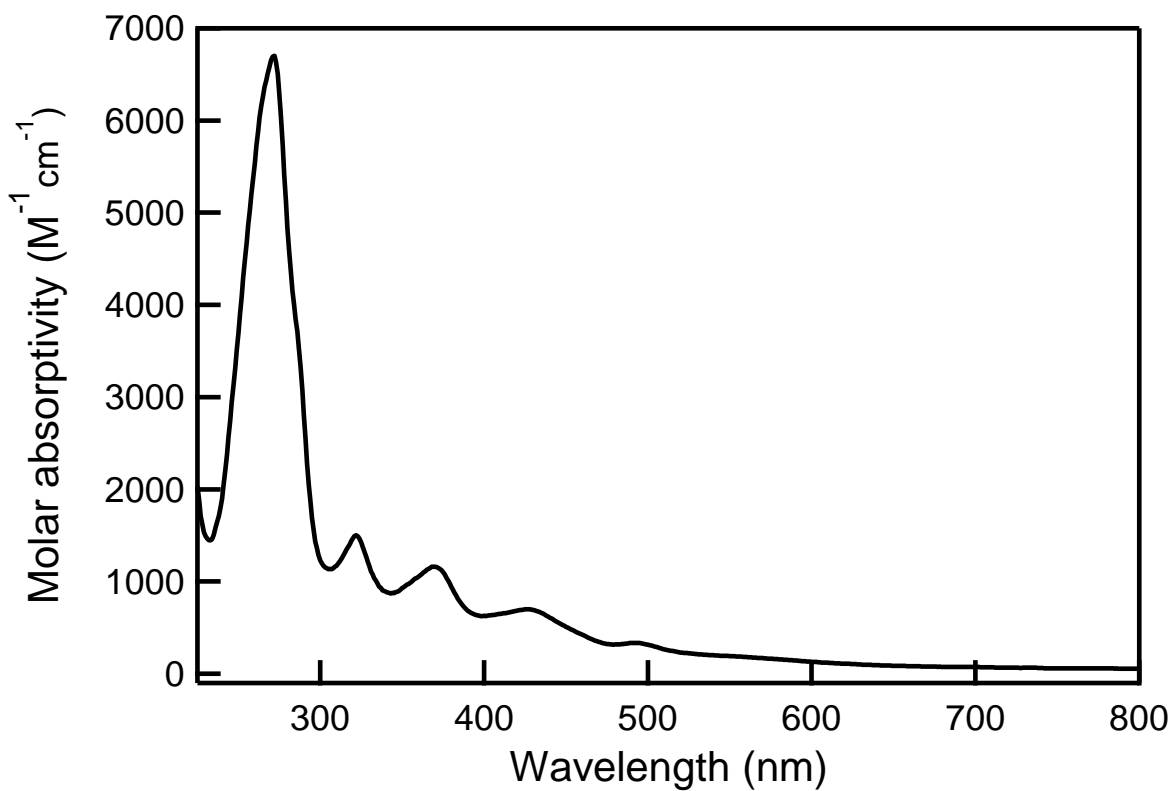
Figure S2. Absorption spectrum of the Blatter radical in DCM (C = 1.4×10^{-4} M) reported in molar absorptivity units.

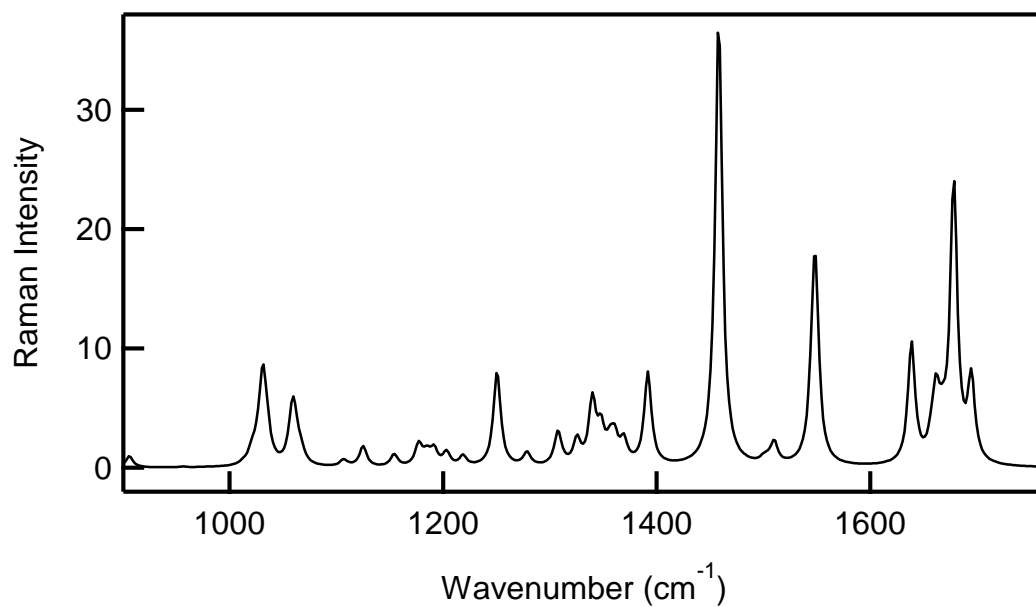## S4. Calculated Raman spectrum of the Blatter radical

Figure S3. Calculated Raman spectrum of the radical, showing the spectral region with the most prominent bands.

S5. Concentration Dependence of Absorption and Fluorescence Excitation Spectra
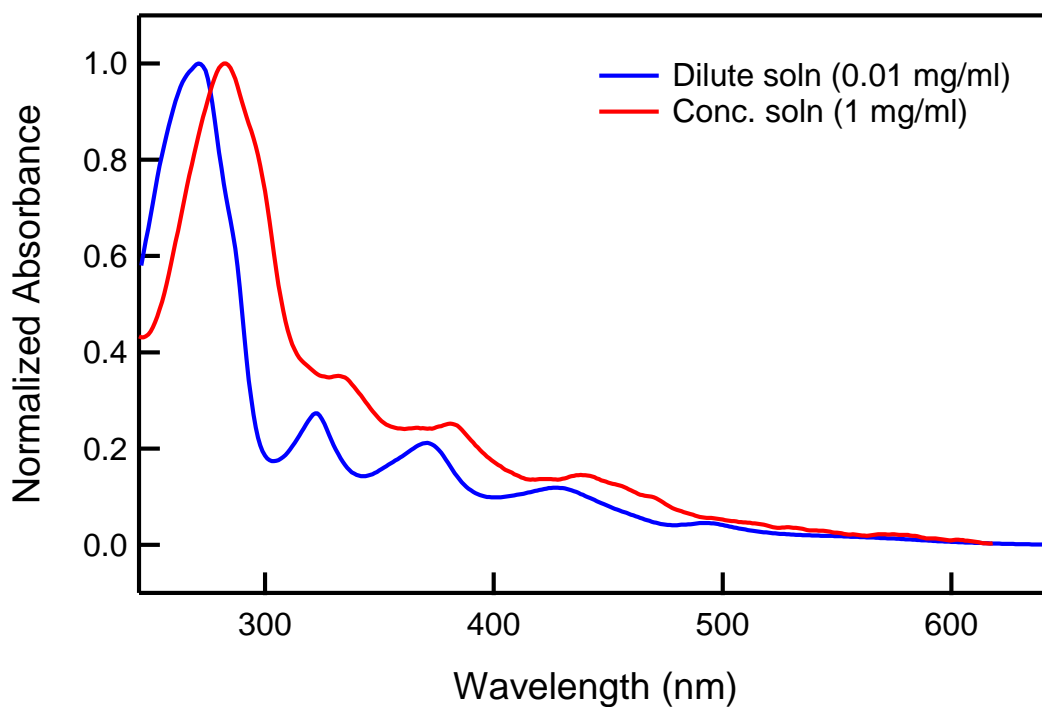

Figure S4. Effect of concentration on the Blatter radical solution absorption spectrum.
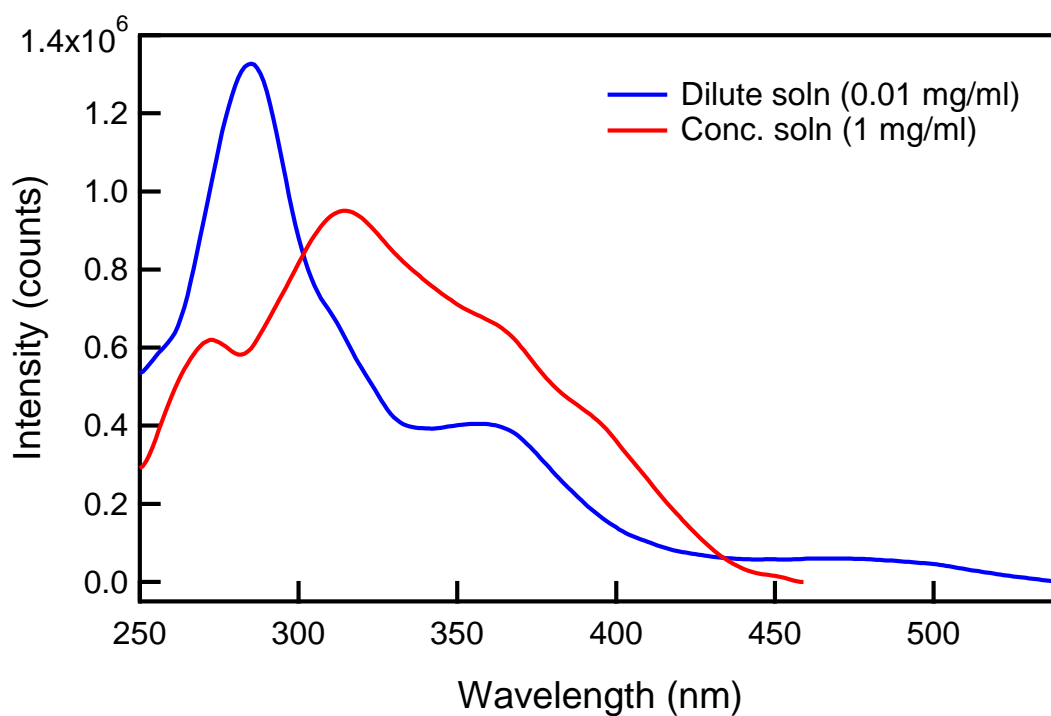

Figure S5. Effect of concentration on the Blatter radical fluorescence excitation spectrum monitored at 595 nm.

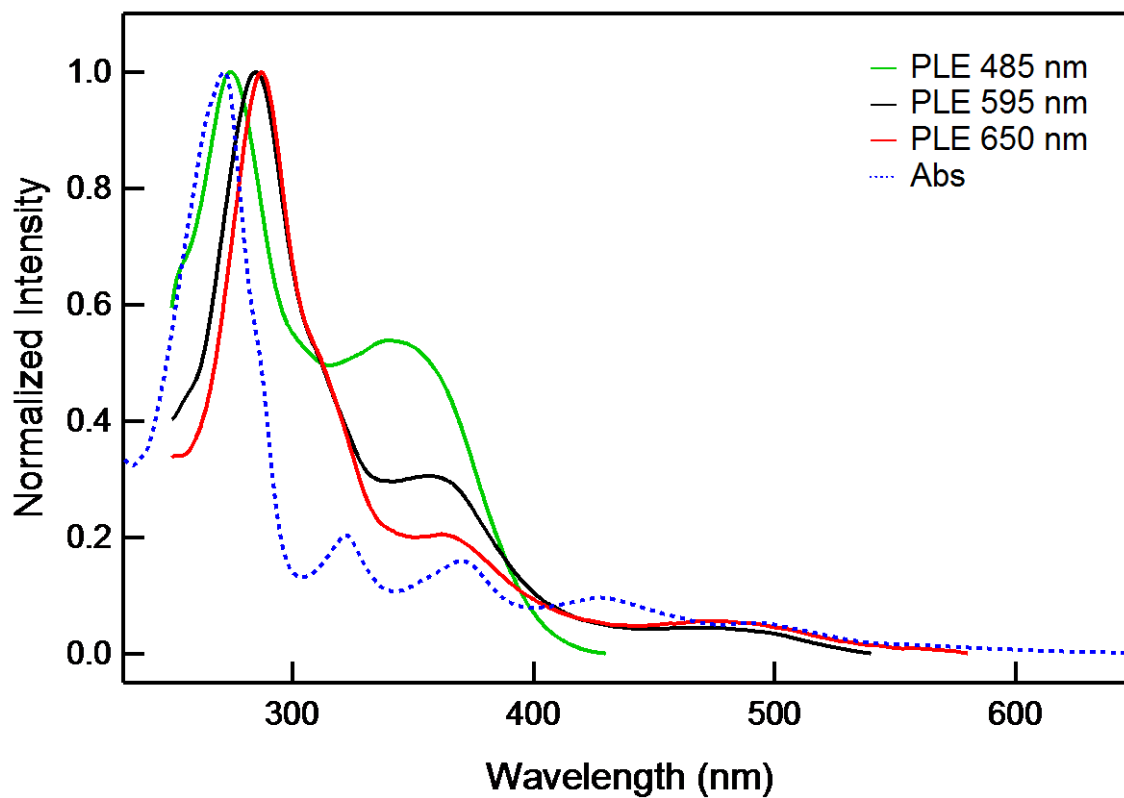**S6. Excitation spectra for the Blatter radical in solution**

Figure S6. Excitation spectra for the Blatter radical in a 0.01 mg/ml DCM solution monitoring the emission at 485, 595 and 650 nm. The blue curve denotes the absorption spectrum of the solution. All the spectra have been normalized for comparison purposes.

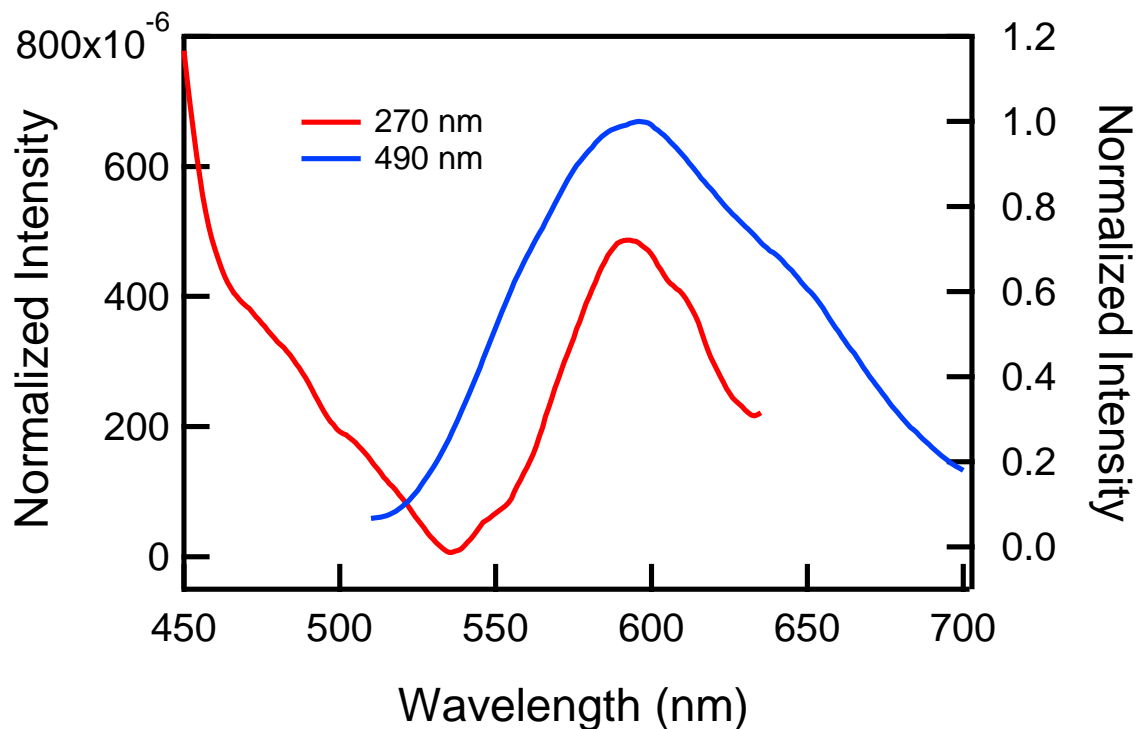**S7. Emission after excitation within the highest absorption band at 270 nm**

Figure S7. Expanded view of the 270 nm excited emission spectrum of a dilute solution of the Blatter radical (red), showing a very week emission band with λ_{max} = 593 nm, similar to the emission band with direct excitation at 490 nm (blue). The existence of this band indicates that internal conversion to the LUMO state occurs with a very small quantum yield (the emission band at 350 nm is normalized to 1).

S8. Stability measurements of the Blatter radical

The stability of the radical compound upon exposure to air and light was probed in several experiments in both the solution and solid state phase. Representative normalized photoluminescence spectra from a neat radical film are included in Figure S3. Negligible variation in the fluorescence spectral and intensity characteristics are observed in consecutive experiments performed under ambient and vacuum conditions. Furthermore exposure to air for a period of 7 days results to a marginal (of the order of 5%) loss in fluorescence intensity and very small variation in the fluorescence lineshape. Similar results have been obtained from the radical in solution form. All the experiments indicate that photo-oxidation and aging effects are rather unimportant within the light intensities and time duration of the spectroscopic experiments of our study.
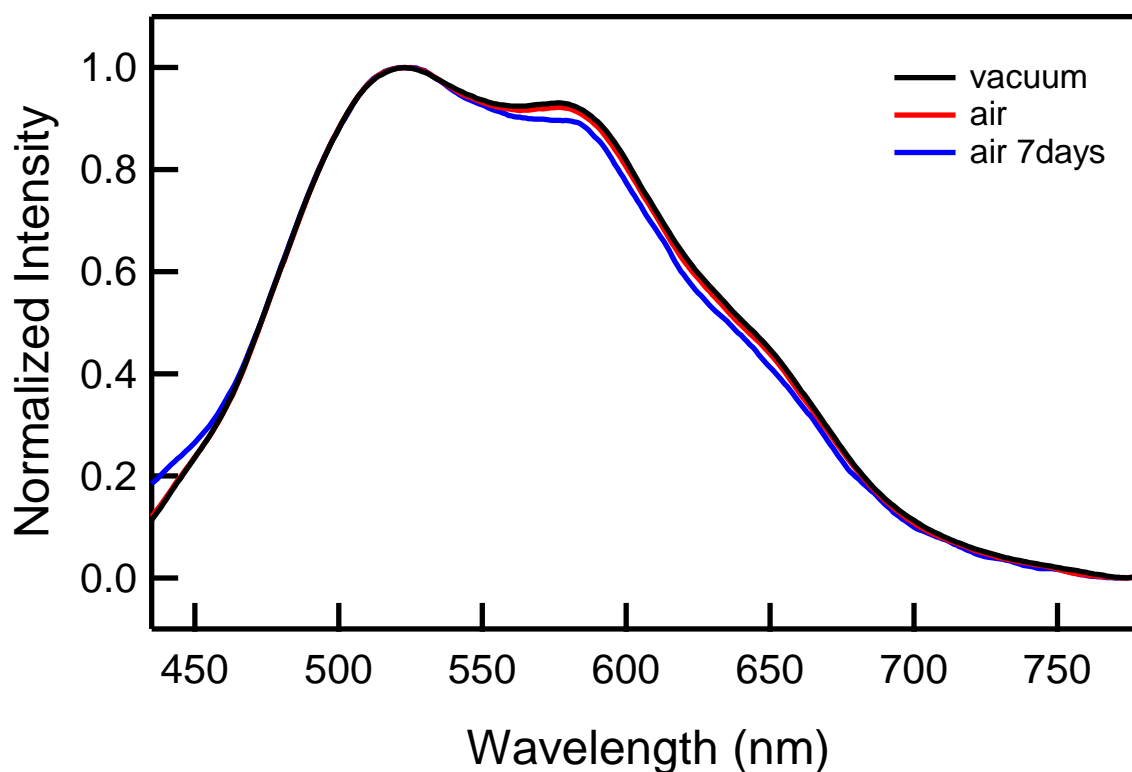

Figure S8. Fluorescence spectra of a Blatter radical neat film with excitation at 405 nm monitored for stability in air and light.

S9. Excitation-dependent Fluorescence Spectra of the Blatter Radical Neat Film
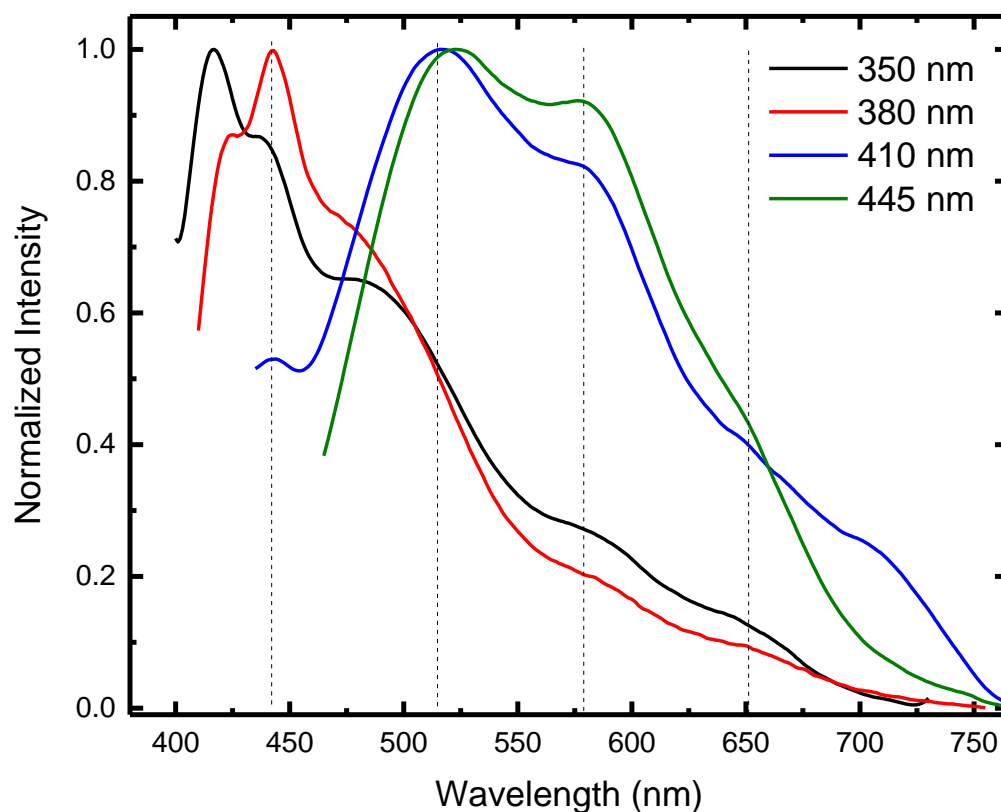

Figure S9. Fluorescence spectra for the Blatter radical neat film (0.1mg/ml DCM solution) as a function of excitation wavelength. The sharp feature at ~445 nm is attributed to quartz substrate emission, as commented in the manuscript. The position of the rest of the emission bands, indicated by the dotted black lines, appears roughly independent of excitation wavelength in the examined 350-450 nm range.

S10. Analysis of time-resolved fluorescence measurements

Table S2. Exponential fit parameters for the time-resolved fluorescence curves.

Excitation (nm)	τ_1 (ns)	τ_2 (ns)	τ_3 (ns)
Solution			
500	1.4	3.26	
550	1.74	4.78	
590	1.93	730	
Pristine Film			
480	0.70	3.11	12.2
580	0.78	3.46	25.8
640	0.82	3.49	22.5
Blend 75:50 Film			
480	0.65	2.52	8.11
580	0.77	3.36	14.2
640	0.69	2.95	9.6
Blend 50:50 film			
480	0.59	2.45	8.77
580	0.60	2.24	7.03
640	0.61	2.38	7.13
Blend 25:75 Film			
480	0.61	3.50	8.45
580	0.78	2.85	7.80
640	0.71	2.73	7.31